Spectroscopic study on transformations of dissolved organic matter in coal-to-liquids wastewater under integrated chemical oxidation and biological treatment process

Siwei Peng[1], Xuwen He[1],*, Hongwei Pan[2]

1. Department of Chemical and Environmental Engineering, China University of Mining and Technology (Beijing), Beijing 100083, China
2. School of Water Conservancy, North China University of Water Resources and Electric Power, Zhengzhou 450045, China

ARTICLE INFO

ABSTRACT

A large amount of wastewater containing various toxic organic contaminants is produced during coal-to-liquids process. In this study, several spectroscopic methods were used to monitor the transformation of organic pollutants during an integrated chemical oxidation and biological process. The results showed that the hydrophobic acid fraction increased after Fenton oxidation, which was likely due to the production of small-molecule organic acids. Soluble microbial products were generated during biological treatment processes, which were degraded after ozonation; meanwhile, the hydrophilic base and acid components increased. Ultraviolet-visible spectroscopic analysis indicated that peaks at the absorption wavelengths of 280 and 254 nm, which are associated with aromatic substances, were detected in the raw water. The aromatic substances were gradually removed, becoming undetectable after biological aeration filter (BAF) treatment. Fourier transform infrared spectroscopy analysis revealed that the functional groups of phenols; benzene, toluene, ethylbenzene, and xylene (BTEX); aromatic hydrocarbons; aliphatic acids; aldehydes; and esters were present in raw wastewater. The organic substances were oxidized into small molecules after Fenton treatment. Aromatic hydrocarbons were effectively removed through bioadsorption and biodegradation after BAF process. Biodegradable organic matter was reduced and finally became undetectable after anoxic–oxic treatment in combination with a membrane bioreactor. Four fluorescent components were fractionated and obtained via excitation–emission matrix parallel factor analysis (EEM-PARAFAC). Dissolved organic matter fractionation in conjunction with EEM-PARAFAC was able to monitor more precisely the evolution of characteristic organic contaminants.

© 2018 The Research Center for Eco-Environmental Sciences, Chinese Academy of Sciences. Published by Elsevier B.V.

Introduction

With the gradual consumption of petroleum resources, much attention has been paid to the coal liquefaction industry worldwide (Huang and Yuan, 2015; Wei and Shi, 2015). Coal-to-liquid (CTL) is a strategic industry for replacing petroleum resources, and thus a measure that can safeguard Chinese energy security. Beyond that, the coal liquefaction industry is not only important for realizing clean and efficient utilization of coal, but also is necessary for improving the quality of fuel oil. Optimization of the production technology of coal-to-oil can promote the transformation and upgrading of the coal

---

industry and help solve the problems regarding coal production capacity and related issues.

The rapid development of the CTL industry in China has brought extensive attention to the treatment of effluent produced *via* coal liquefaction. CTL processes generate a large amount of wastewater, which characteristically has a high organic concentration and low biodegradability. The chemical oxygen demand (COD) of this wastewater is generally around 9000–10,000 mg/L. In addition, CTL wastewater is very complex in its chemical composition of organic matter and contains many toxic and bioresistant organic substances, such as hydrocarbons, aldehydes, phenols, and benzenes.

The characteristics of the dissolved organic matter (DOM) in wastewater affect the treatability and process options for the wastewater (Jiang et al., 2017). Because of the complex constituents of DOM in CTL wastewater, traditional biological processes alone are unable to purify wastewater effectively, so combined physicochemical and biological processes are always used for such wastewater (Yue et al., 2015; Sahu et al., 2017). Actually, integrated processes have been established and operated for many years in China for CTL wastewater treatment. In particular, desulfurization, dephenolization, and deamination pretreatments are conducted first for separation of sulfide ions, phenols, and ammonium, respectively (Hou et al., 2014; Han et al., 2010a, 2010b). After that, Fenton oxidization is used to detoxify the wastewater and improve its biodegradability (Peng et al., 2016), and then the wastewater is treated further *via* an efficient biological aeration filter (BAF). To remove the residual organic matter in the wastewater, an integrated ozonation preoxidation and anoxic–oxic (A/O) process is applied (Nawrocki and Kasprzyk-Hordern, 2010; Barker and Stuckey, 1999; Deng et al., 2017). Finally, the A/O effluent is treated in depth by a membrane bioreactor (MBR) for water reclamation.

At present, most of the CTL wastewater in China conforms to the emission standard after such treatment, but the effluent might contain some toxic substances at trace concentrations. Few studies have focused on the monitoring and evaluation of these trace toxic organic pollutants in CTL wastewater treatment (Lu et al., 2006), yet most of these substances have carcinogenic, teratogenic, and mutagenic effects and pose a great threat to ecological security and human health. In addition, it has been difficult to observe the changes undergone by organic pollutants during the actual treatment of CTL wastewater. Therefore, it was necessary to find a simple and effective method to monitor the characterization of the changes in organic pollutants during CTL wastewater treatment processes.

Spectroscopic methods have been widely used for characterization of dissolved organic contaminants in wastewaters from different industrial sources. Li et al. (2017) investigated the migration and transformation of organic compounds in wastewater from physicochemical treatment processes by using different spectroscopic methods. They applied ultraviolet absorbance (UVA) and fluorescence techniques to assess the formation of biodegradable dissolved organic carbon (BDOC) and bromate during ozonation and suggested that measurement of UVA was able to assess the formation of BDOC and bromate. They employed LED ultraviolet (UV) fluorescence sensors to monitor DOM online to predict the formation potential of disinfection by-products (DBPs) during water disinfection treatment. It was found that both protein-

like and humic-like fluorescence can be excited by UV_{280} LED and then detected *via* photodiodes combined with light filters (350 ± 15 nm and 440 ± 30 nm, respectively) and that the UVA at 280 nm can substitute for the UVA at 254 nm for online monitoring of DOM and for predicting DBP formation potential (Li et al., 2016). Fluorescence analysis combined with parallel factor analysis (PARAFAC) is widely used to predict the transformation of typical DOM in water treatment processes or in aquatic environments. Li studied the changes in DOM during municipal wastewater treatment using fluorescence analysis and PARAFAC (Li et al., 2014). In addition, Osburn et al. (2012) combined excitation–emission matrix (EEM) fluorescence and PARAFAC analysis to model base-extracted particulate organic matter (POM) and DOM compositions in the Neuse River Estuary (NRE). It was demonstrated that four PARAFAC components (C1–C3 and C6) were derived from terrestrial sources to the NRE, one component (C4) was enriched in the POM and in surface sediment pore water DOM, and one component (C5) was related to recent autochthonous production. Sgroi et al. (2017) used EEM and different data processing methods, including peak-picking methods, Fourier transform infrared (FT-IR) analysis, and PARAFAC, to evaluate their suitability for producing effective surrogate pollutant indices. Use of a convenient and sensitive fluorescence analytical technique as a monitoring tool could quickly reveal the removal and conversion of organic compounds in different water bodies.

As mentioned above, CTL wastewater contains different kinds of harmful organic contaminants, but few studies have focused on the transformation of these pollutants at the molecular level throughout the wastewater treatment process. In this study, we combined the methods of UV spectroscopy, FT-IR spectroscopy, and EEM fluorescence spectroscopy to systematically investigate the molecular structure and transformation of organic components during an integrated treatment process for CTL wastewater. In addition, gas chromatography–mass spectrometry (GC–MS) was conducted to analyze the variation of organic matter in CTL wastewater and verify the accuracy of the spectroscopic analysis (Appendix A Fig. S9 and Table S1). The objective of this study was to gain insight into the transformation mechanisms of organic pollutants in different wastewater treatment stages and to evaluate the operating efficiency of the integrated process for CTL wastewater treatment.

1. Materials and methods

1.1. Collection of samples

The CTL wastewater was collected from a coal liquefaction plant in China. This plant is the first megaton engineering project using direct coal liquefaction technology and has been operating stably for 9 years. The specific process of its sewage treatment plant is presented in Fig. 1. Wastewater samples were collected from the influent, Fenton oxidation stage, BAF effluent, ozonation stage, A/O effluent, and MBR effluent, three times a day, *i.e.*, morning, noon, and night, from April 6 to 26, 2017. The wastewater samples were stored in brown glass bottles, which had been washed with acetone and
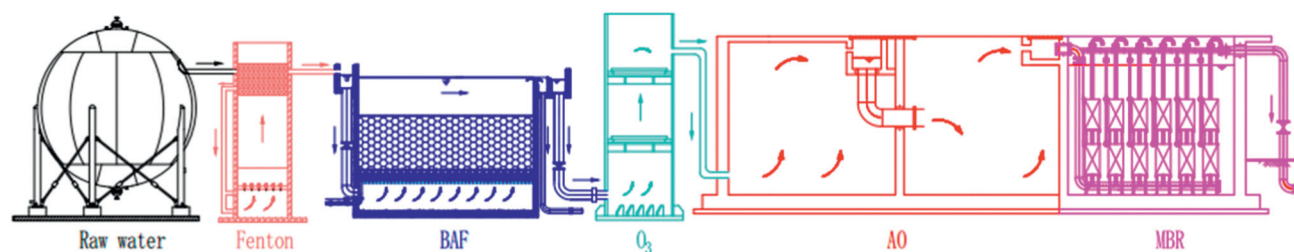
Fig. 1 – Coal-to-liquids wastewater treatment process.

ultrapure water and dried in advance. Then, the water samples were brought back to the laboratory and stored in a 4°C refrigerator. The samples were used for further analysis and the average value was presented as the experimental result.

1.2. Analytical methods

1.2.1. Water quality analysis
The water quality was analyzed following APHA-AWWA-WEF (1998) Standard Methods. Chemical oxygen demand (COD) concentrations were determined using the potassium dichromate method. Biological oxygen demand (BOD) concentrations were determined via the dilution inoculation method, which is suited for water samples whose BOD levels are greater than 2 mg/L but not more than 6000 mg/L. The values of pH were measured with a PHS-3C precision pH instrument (LeiCi, Shanghai, China). The total phosphorus (TP) concentrations were determined by the ammonium molybdate spectrophotometric method. To measure total nitrogen (TN) concentrations, predigestion of the water samples was performed with alkaline potassium persulfate, and then NO_3^- was measured via UV spectrophotometry at the wavelength of 254 nm. Ammonia nitrogen (NH_4^+-N) concentrations were analyzed using Nessler's reagent spectrophotometry. The water quality of the samples collected from different wastewater treatment stages is given in Table 1.

1.2.2. DOM fractionation procedure
The separation process of DOM is shown in Fig. 2. The resins used for separation of the DOM in the effluents were nonionic-type XAD-8 adsorption resin, DOWEX50-type cation exchange resin, and IRA958-type anion exchange resin. DOM resin separation was conducted based on the methods reported by Imai et al. (2002) and Kitis et al. (2002). According to the

enrichment and elution of DOM components by the different resins, the DOM of the effluent samples was fractionated into hydrophobic acid (HoA), hydrophobic base (HoB), hydrophobic neutral (HoN), hydrophilic acid (HiA), hydrophilic base (HiB), and hydrophilic neutral (HiN) components.

1.2.3. DOM characterization
A UV–visible (UV–vis) spectrophotometer (UV-2800, Shanghai Younike) was used. The water samples were diluted tenfold with ultrapure water, and the sample pH was adjusted to 7. The UV–vis spectroscopy was performed with ultrapure water as the control. The scanning conditions were as follows: wavelength range was 200–600 nm, data acquisition precision was 0.5 nm, and the cuvette used was a 1 mL quartz cell (Louvet et al., 2013).
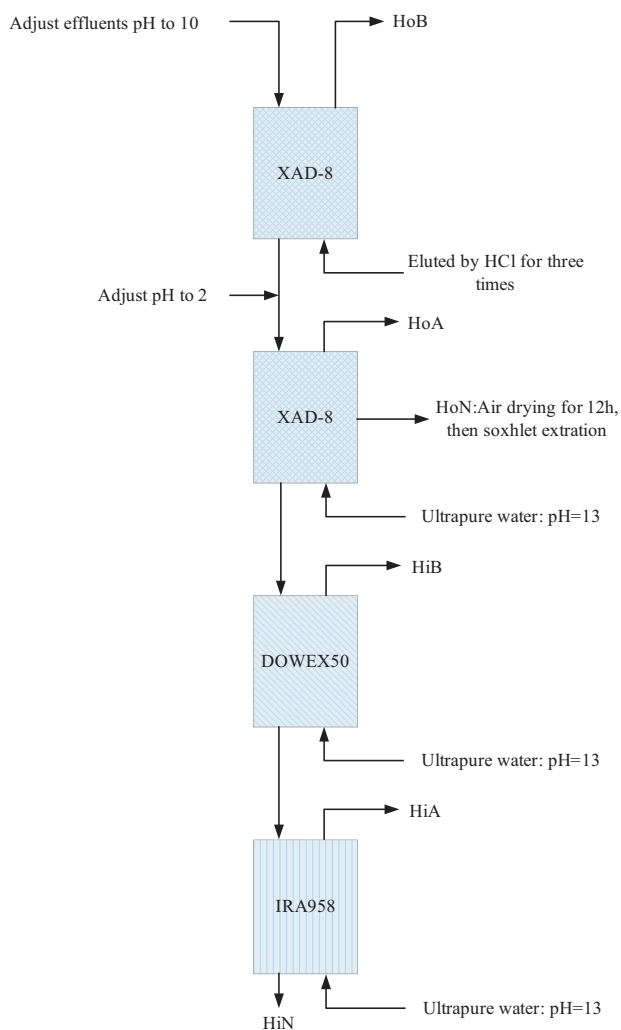
The Nicolet Nexus 410 spectrometer was used to obtain the FT-IR spectra of the water samples. First, the water samples were dropped on a glass sheet, and then dried for 18 hr at a cool temperature. Next, the solid materials on the glass were ground with potassium bromide grinded pressed into tablets for testing. The wavelength range was 400–4000 cm^{-1}, the spectrograph resolution was 2 cm^{-1}, and the signal to noise ratio (SNR) was 50,000:1 (Yang et al., 2015).

A Hitachi F-7000 fluorophotometer was used to measure 3D-EEM fluorescence. The pH values of the water samples were adjusted to 2 before testing in order to eliminate the influence of complexation between metal ions and organic compounds. Ultrapure water was used as a blank water sample. Testing conditions were as follows: a 150 W xenon lamp was used as the source, the PMT voltage was 400 V, the excitation (Ex) scanning wavelength was 200–400 nm, the emission (Em) scanning wavelength was 220–550 nm, the Ex and Em slit width was 5 nm, the Ex and Em wavelength scan interval was 5 nm, and the scanning velocity was 12,000 nm/min (Cheng et al., 2018).

Table 1 – Effluent indices of different treatment stages.						
Water sample	COD	BOD$_5$	TN	NH_4^+-N	TP	pH
	(mg/L)	(mg/L)	(mg/L)	(mg/L)	(mg/L)	
Raw water	5849 ± 19.91	4541 ± 12.25	374 ± 7.65	98.6 ± 1.60	1.82 ± 0.20	9.02 ± 0.20
Fenton	2745 ± 7.62	1223 ± 5.33	207 ± 1.27	52.3 ± 4.24	0.47 ± 0.20	9.55 ± 0.20
BAF	1858 ± 11.10	827 ± 9.14	164 ± 4.22	39.1 ± 0.77	0.38 ± 0.06	7.16 ± 0.20
O$_3$	764 ± 9.26	389 ± 14.90	129 ± 4.80	22.52 ± 0.43	0.34 ± 0.11	8.12 ± 0.20
A/O	233 ± 3.31	55.5 ± 13.30	67 ± 2.77	9.19 ± 1.00	0.24 ± 0.03	8.15 ± 0.20
MBR	25 ± 3.96	2.7 ± 0.29	6.1 ± 0.23	3.2 ± 0.32	0.06 ± 0.03	7.82 ± 0.20
COD: chemical oxygen demand; BOD: biological oxygen demand; BAF: biological aeration filter; MBR: membrane bioreactor.						

Fig. 2 – Schematic diagram of the procedure for dissolved organic matter (DOM) fractionation.

For GC–MS analysis, the water samples were filtered through a 0.45 μm glass fiber membrane to remove particulates. Then, 5 g NaCl was added to the 200 mL water sample. Liquid–liquid extraction was done with 50 mL of chromatographic grade dichloromethane and 50 mL of chromatographic grade *n*-hexane, respectively, and the extraction system was agitated for 20 min. Anhydrous Na_2SO_4 was used to consolidate the organic phases, which were then rotary evaporated to 2 mL. The main parameters are as follows: The minimum matching factor was set at 80 in library searching. The analysis type was set as Sample, mass-to-charge ratio scanning range set as Auto, constituent peak width set as 12, adjacent peaks offset set as One, and resolution rate set as Medium. GC/MS analysis was conducted by using a GCMS-QP2010Plus system (Shimadzu). A DB-5MS capillary column from Agilent (30 m × 0.25 mm × 0.25 μm) was used with splitless injection of samples. Helium gas was used at a constant linear velocity of 40 cm/sec. Other experimental conditions were as follows: the drying gas velocity was set as 6 L/min; injection port temperature was 250°C; electron energy was 70 eV; ion source temperature was 200°C; transmission line temperature was

300°C; scanning range was 45–600; temperature was increased from 40 to 310°C at a rate of 8°C/min, and then was kept at 310°C for 5 min; injection volume was 1 μL; and split ratio was 10:1 (Collard et al., 2015).

1.3. Data processing

PARAFAC analysis was based on the theory of trilinear decomposition (Zhang et al., 2011). This method identifies the fluorescence peak number, type of fluorescence, and fluorescence intensity (Aftab and Hur, 2017; Yang et al., 2017; Maqbool and Hur, 2016; Oloibiri et al., 2017). The fluorescence intensity after PARAFAC analysis was expressed in Raman correction units (R.U.). The drEEM 2.0 toolkit developed by Murphy was used in this PARAFAC analysis method, and the operating system is MATLAB R2014a (Lenhardt and Dramićanin, 2016). The PARAFAC components were validated by split-half analysis in which the outliers with negative values had been removed. The results are shown in Appendix A Fig. S1.

2. Results and discussion

2.1. DOM fractionation

As shown in Fig. 3, HoB was the largest proportion fraction, accounting for 28.31% of DOM in the raw water. The proportions of HoA, HoN, HiA, HiB, and HiN were 13.73%, 14.35%, 14.01%, 11.91%, and 17.69%, respectively. In total, hydrophobic substances accounted for 56.39%, which was slightly higher than the proportion of hydrophilic materials, at 43.61%. Based on the information presented in **Appendix A Table S1**, hydrophobic substances in the raw water are probably related to PAHs and benzene, toluene, ethylbenzene, and xylene (BTEX), and the hydrophilic materials are likely associated with phenols, aldehydes, alcohols, *etc*.

After Fenton treatment, there were marked changes in the proportions of the HoA and HoB fractions, as the HoB ratio decreased by 19.38% and the HoA ratio increased by 12.36%. It was likely that a portion of hydrophobic organic contaminants in the raw water, such as benzenes and aromatic compounds, was partially removed and converted into small-molecule organic acids during Fenton oxidation (Li et al., 2012). After BAF treatment, the HoN fraction increased significantly from 19.46% to 69.8%, likely because soluble microbial metabolites (SMMs), which are always related to tryptophan-like proteins, were produced by microorganisms and finally remained in the form of HoN components. In addition, these protein-like substances and microbial metabolites are removed by O_3 oxidation, thus the HoN component decreased; meanwhile, the relative ratio of the HiA and HiB components increased. In A/O treatment, biodegradable fractions such as HiA and HiB were removed, while SMMs were generated; hence, the biodegradable fractions were presented in the form of the HoN component and increased again. Finally, the organic matter including SMMs, organic acids, and trace organic contaminants in the MBR effluent was thoroughly mineralized into H_2O and CO_2, and low concentrations of organics were retained. The following analysis was performed to investigate the transformation of organic components in different fractions.
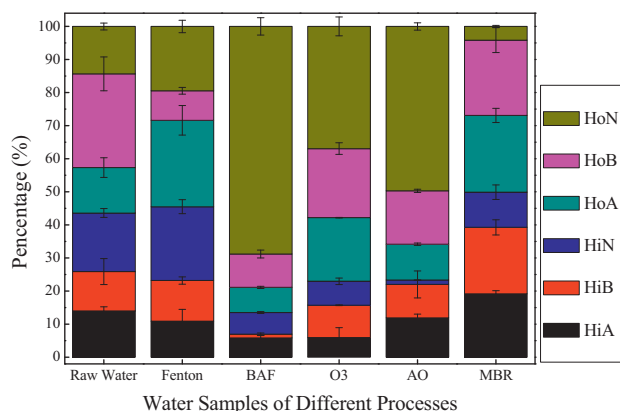
Fig. 3 – DOM distribution in water samples from different processes.

2.2. UV–visible spectroscopy

From Appendix A Fig. S2, it can be observed that the raw water appeared brownish black, the Fenton effluent was light brown, and the other water samples were colorless. As can be seen from Fig. 4, an absorption peak at 490 nm was present in the raw water and Fenton effluent, but was not detected after BAF treatment, which was consistent with the differences in color. In addition, absorption peaks at wavelengths of 280 nm and 254 nm, which are related to organic matter containing π–π conjugated double bonds, such as C═C and C═O, were detected in the raw water and Fenton-treated water. These characteristic peaks indicated the possible presence of benzenes and phenols in the water samples. After BAF treatment, the absorption peaks at 280 nm and 254 nm decreased and finally disappeared, revealing that the benzenes and phenols were gradually removed. In addition, it was observed that the intensity of the absorption peak at 210 nm decreased gradually during the integrated treatment process. This characteristic peak is generally associated with C–OH, which was present in most of the organic compounds,
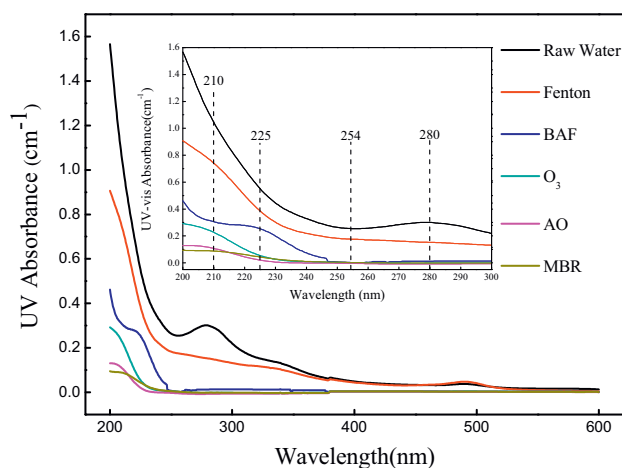
illustrating that the organic concentration in the wastewater was gradually lowered—an observation that was in agreement with the COD analysis. Additionally, it was noted that the absorbance at the wavelength of 225 nm, which is associated with protein-like substances, was clearly present in the BAF effluent and was significantly lower after ozonation, demonstrating that protein-like substances were gradually removed after ozonation treatment. These protein-like compounds mainly originated from bacterial metabolism in the BAF, but also were produced in the A/O and MBR processes with significantly lower absorbance, indicating they were gradually removed and almost disappeared in subsequent treatment steps.

2.3. FT-IR spectroscopic analysis

The characteristic functional groups and specific molecular structures of organic compounds in water samples can be identified *via* infrared spectroscopic analysis. As shown in Fig. 5, there were seven absorption peaks in all the water samples, and the characteristic functional groups corresponding to different wavelengths are summarized in Table 2, according to the literature (He et al., 2008; Bu et al., 2010).

The chemical composition of the raw wastewater was very complicated. Six absorption peaks were detected, *i.e.*, peaks 1, 2, 4, 5, 6, and 7, indicating that the functional groups of phenols, BTEX, aromatic hydrocarbon, aliphatic acids, aldehydes, and esters, respectively, were present in the raw wastewater. Most of these organics likely originated from the pyrolysis of coal. It was observed that peak intensity in the range 3300–3600 cm^{-1} for the MBR effluent was obviously weakened. This characteristic peak is related to phenols and alcohols, revealing that MBR treatment performed well in the removal of phenols and alcohols. After Fenton treatment, the peak 7 intensity was enhanced, revealing that the raw organic matter had been oxidized into small molecules, such as aldehyde and/or ketone. C═C stretching (peak 6) of aromatic hydrocarbons was found in the raw water and Fenton effluent, but disappeared after BAF treatment. Aromatic hydrocarbons
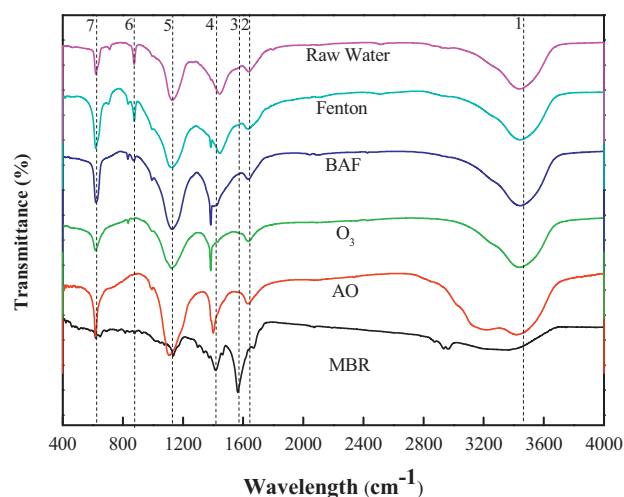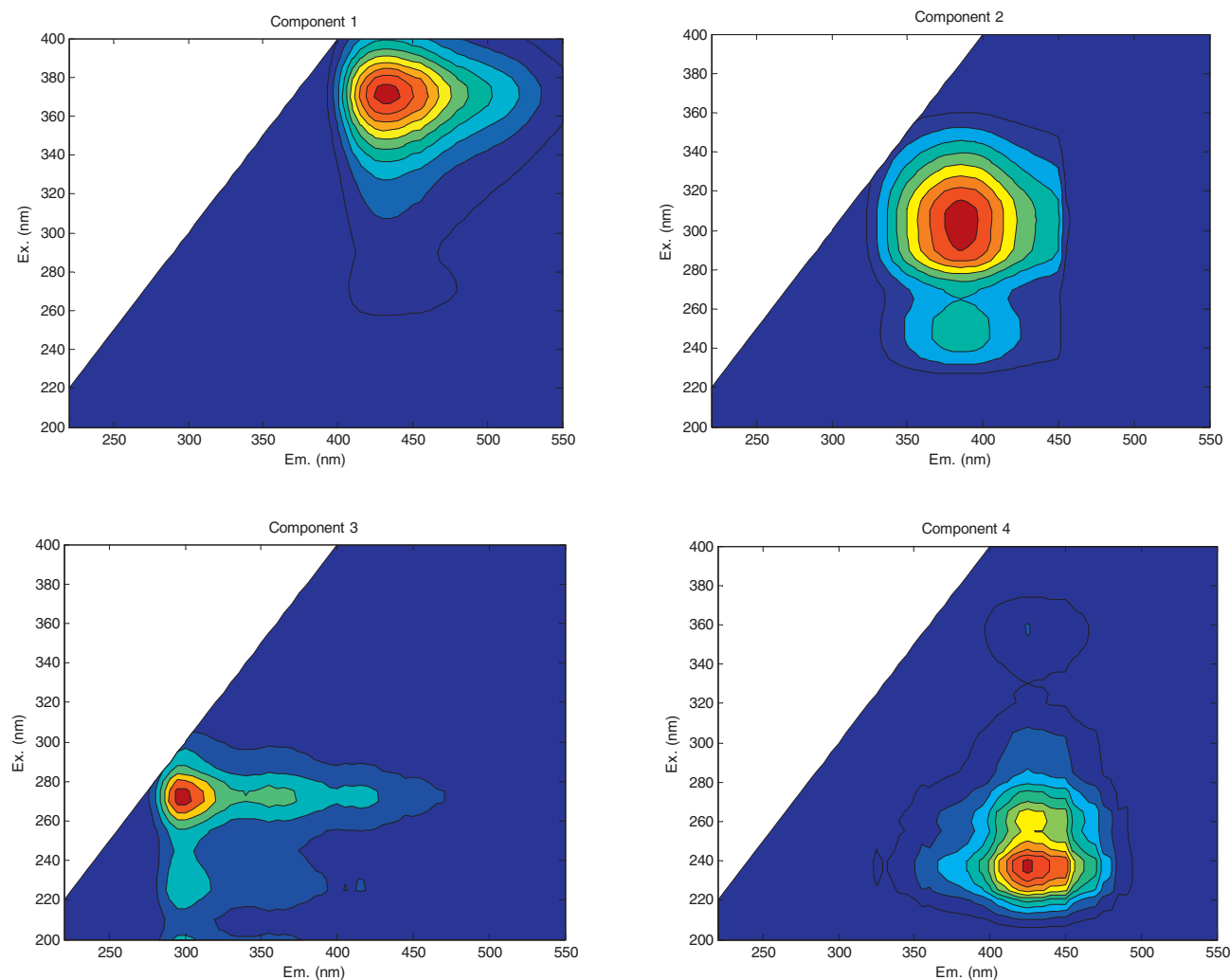

Fig. 4 – UV–visible spectroscopic characteristics of water samples.

Fig. 5 – Fourier transform infrared spectra of the different water samples.

Table 2 – General assignments of FT-IR spectra of DOM fractions.

Peak no.	Wavelength (cm^{-1})	Assignment
1	3600–3300	O-H stretching of hydroxyl groups from hydrogen bonding; N-H vibration of amidocyanogen
2	1690–1580	C=O stretching of amide groups; Aromatic C=C double bonds that are conjugated with C=C of COO–; C=O vibration of quinone
3	1465–1440	Carboxylic acid in-plane C–O–H bending; Aliphatic C–H deformation
4	1420–1390	O–H vibration of carboxylic group; C–H deformation abutted upon C=O
5	1150–1100	C–O stretching of esters
6	900–850	C=C stretching of arene
7	650–550	C–C=O vibration of aldehyde or ketone; C–Cl stretching of halohydrocarbon

biodegradation, as extracellular polymeric substances (EPSs) are the major constituents of biofilms. Nonpolar aromatic hydrocarbons are typical nonpolar molecules; therefore, they could be removed more readily through hydrophobic interactions between EPSs and aromatic hydrocarbons. The characteristic peak of carboxyl compounds and/or aliphatic acid was present in all samples, as much organic matter contains carboxyl groups, such as protein-like substances and various organic acids. The protein-like substances primarily originated from bacterial activity in the biological treatment processes. The source of organic acids was very complex, as they were likely produced *via* coal pyrolysis, chemical oxidation, and biological degradation. In addition, a peak observed in the wavelength range of 1150–1100 cm^{-1} usually indicates esters, which also are generated from the coal pyrolysis process. The intensity of the peak due to esters weakened throughout the wastewater treatment and finally was undetectable after the MBR process.

generally are resistant to chemical oxidation, so most of them were retained after Fenton oxidation. The mechanisms of the aerobic biofilm process were attributed to bioadsorption and

Fig. 6 – Four components identified by the Excitation–emission matrix parallel factor analysis.

2.4. DOM fractionation in combination with EEM-PARAFAC

The EEM contours of the fractionated water samples from different treatment processes are given in Appendix A Figs. S3–S8. The EEM-PARAFAC model was used to divide all the water samples into four fluorescence response regions, and then semiquantitative analysis was carried out. The four fluorescent components, *i.e.*, component 1 (C1), component 2 (C2), component 3 (C3), and component 4 (C4), are shown in Fig. 6, at positions Ex/Em = 380 nm/430 nm; Ex/Em = 300 nm/390 nm; Ex/Em = 275 nm/300 nm; and Ex/Em = 240 nm/360 nm, respectively.

The possible organic matter compounds present in each component are summarized and listed in Table 3. C1 was possibly related to humic substances and benzopyrene; C2 was associated with p-π conjugation of benzenediamine, toluidine, benzopyrene, and quinhydrone; C3 was attributed to π-π conjugated groups of aromatic substances, such as BTEX, benzenediamine, toluidine, naphthalene, quinones, and soluble microbial products (SMPs) mainly composed of aromatic proteinaceous substances; and C4 was probably associated with fulvic acid.

From Fig. 7a and Appendix A Fig. S3a, it was found that C1, C2, C3, and C4 were present in the EEM fluorescence spectrum of the CTL raw water in proportions of 16.3%, 9.8%, 37.9%, and 36.0%, respectively. C3 and C4 are the dominant fractions, indicating the presence of various organic compounds in the wastewater, including humic substances, benzopyrene, anilines, aromatic substances, and fulvic acid, which can be confirmed *via* the GC/MS analysis (Appendix A Table S1). These large proportions of C3 and C4 show that BTEX, phenols, and fulvic acid might be the main pollutants in the CTL raw water. It can be seen from Fig. 7a and Appendix A Fig. S4 that, after Fenton treatment, the fluorescence intensities of C1 and C4 were reduced by 9.9% and 31.3%, respectively, whereas those of C2 and C3 were enhanced by 36.2% and 5.0%, respectively. This result indicated that BTEX, organic amines, phenols, and fulvic acid were partially removed. BTEX, anilines, and phenols could be easily converted into other organic compounds (organic acids, ketones, and quinones) under Fenton oxidation (Zhang et al., 1995; Hara, 2017; Xue et al., 2018), as quinone and quinhydrone are widely detected as intermediates of aromatic substances (Liu et al., 2016; Benito et al., 2017). It was noteworthy that the enhancement of

fluorescence intensity of C2 and C3 did not suggest an increase in organic amines, BTEX, or PAHs, but rather the generation of quinhydrone and benzoquinone under oxidative treatment (Marquès et al., 2017; Ge et al., 2016). After BAF treatment, C1 increased from 6.4% to 25.3% and C3 decreased from 42.9% to 26.7%. Owing to high nonpolarity and low biodegradability, the BTEX and PAHs could be partially removed by activated sludge through bioadsorption, and the phenols could be biologically mineralized into CO_2 and H_2O. In addition, biological treatment produced SMMs mainly composed of tryptophan-like proteins and humic substances, which resulted in high fluorescence intensity in C1 and C3. After ozone oxidation treatment, the proportions of C2 and C3 were high at 29.3% and 31.7%, respectively, indicating that quinhydrone and benzoquinone were also produced during the ozonation process. Because BTEX, humic substances, and fulvic acid are always resistant to chemical oxidation, they were retained in the ozonation effluent. After the A/O process, the proportions of C1, C2, and C4 were greatly reduced and C3 became the most abundant fraction in the effluent. This result revealed that most of the organic pollutants were removed through biological absorption and degradation while microbial metabolites and protein-like substances were being produced. Finally, as observed in Appendix A Fig. S8a, C1, C2, C3, and C4 almost completely disappeared after MBR treatment, which indicated that the harmful organic matter in the effluent was almost completely removed. Organic acids and esters were retained in the final effluent (Appendix A Table S1).

Fig. 7b shows the fluorescent components in different DOM fractions during the wastewater treatment. The organic matter content in the four components gradually decreased, indicating that the integrated process performed well in removing the organic pollutants in the wastewater. C1 was present in the form of HiN, HiA, and HoB fractions in the raw wastewater, whereas the fluorescent intensity of C1 in the HiB and HiA fractions increased after Fenton oxidation. C1 in HoN was likely related to benzopyrene, whereas that in HiA and HiB was attributed to humic substances. This result indicated that hydrophobic compounds with high molecular weight, such as humic substances, were converted into smaller hydrophilic organic molecules. After BAF treatment, the fluorescent intensity of C1 in HoN was greatly enhanced, which was likely owing to humic substances produced by microorganisms. It can be inferred that the physicochemical

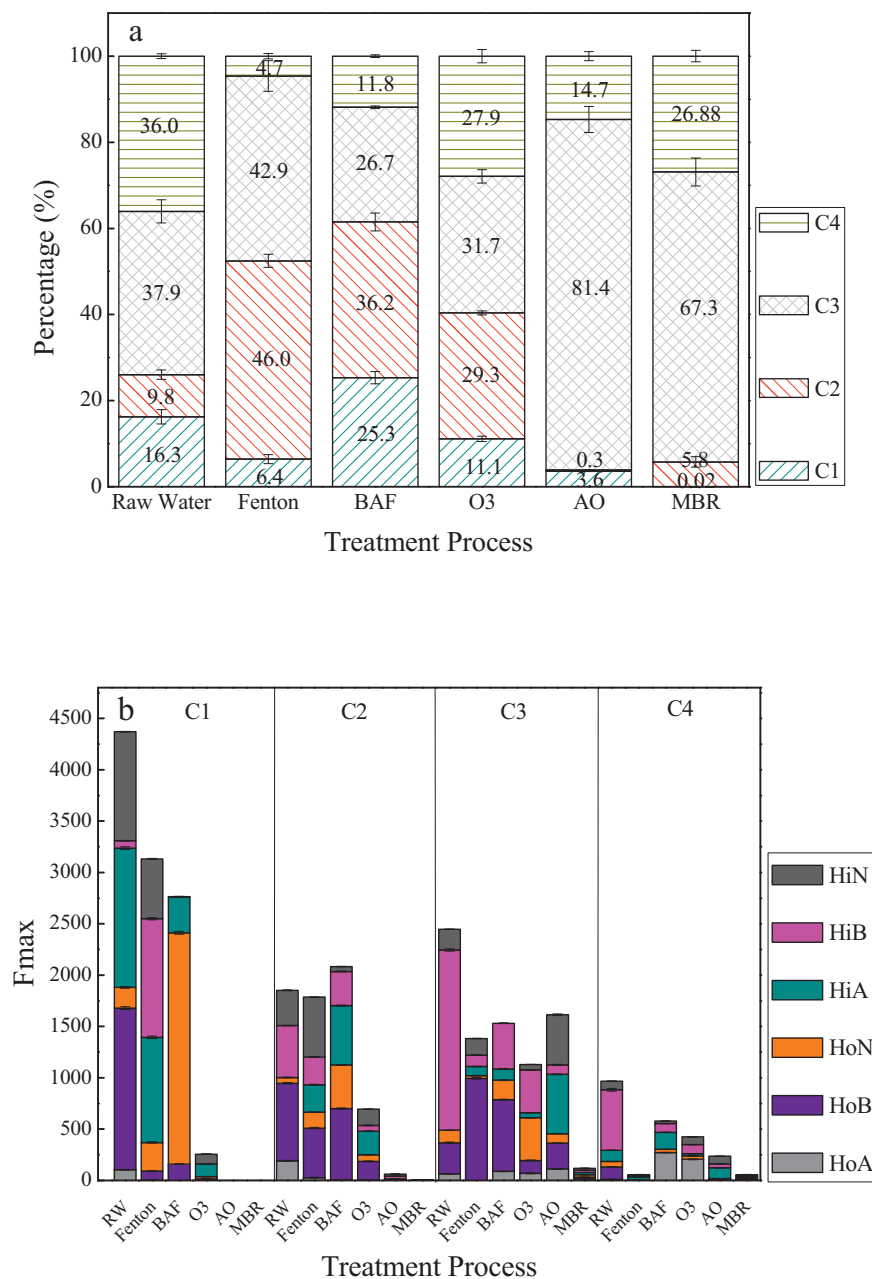| Table 3 – Fluorescence response partitioning of representative organic compounds.		
Component	Organic compounds and Ex/Em maxima	References
C1	Humic substances (Ex/Em = 330 nm/450 nm)	Chen et al. (2003)
	PAHs: Benzopyrene (Ex/Em = 416 nm/469, 493 nm)	Chen et al. (2012)
C2	Quinones: Quinhydrone (Ex/Em = 320 nm/420 nm)	Jiang et al. (2012)
	Organic amines: Aniline (Ex/Em = 320 nm/340 nm)	Wang et al. (1995)
	Benzenediamine (Ex/Em = 335 nm/360 nm)	Wang et al. (1995)
	Toluidine (Ex/Em = 330 nm/350 nm)	Wang et al. (1995)
	Ketones: Acetone (Ex/Em = 300 nm/390 nm)	Han et al. (2010a, 2010b)
C3	Benzenes: BTEX (Ex/Em = 210 nm/280 nm, 260 nm/285 nm)	Bai et al. (2016), Feng et al. (2015)
	Phenolic compounds: Phenol (Ex/Em = 272 nm/300 nm)	Wang et al. (2010a, 2010b)
	Quinones: Benzoquinone (Ex/Em = 275 nm/320 nm)	Jiang et al. (2012)
	Soluble microbial products: Tryptophan proteins	Chen et al. (2003)
	PAHs: Naphthalene (Ex/Em = 280 nm/340 nm)	Yan et al. (1995)
C4	Fulvic acid (Ex/Em = 240 nm/420 nm)	Chen et al. (2003)

Fig. 7 – Change in intensity of the four fluorescent components under the integrated treatment process. (a) Relative percentages of the four components in the six process effluents. (b) Relative percentage of the four components based on the DOM fractionation results.

properties of humic substances from different sources were characterized by distinct hydrophilic–hydrophobic properties. The fluorescent intensity of C1 was greatly weakened after O_3 oxidation, and then disappeared after A/O treatment. The C2 component was related to aniline, benzenediamine, toluidine, quinhydrone, and ketone, the first three of which are basic organic compounds, whereas the quinhydrone and ketones were related to HiA and HiN, respectively. The C2 intensity in HoB and HiB decreased and that in HiN increased after Fenton oxidation, which indicated that aniline was oxidized and removed and that ketones were generated at the same time. The BAF performed well in ketone removal and caused a

decrease in the C2 intensity in the HiN fraction. Likewise, the C2 intensity in all the fractions was greatly reduced after ozonation treatment. As mentioned above, the C3 component was related to BTEX, phenolic compounds, tryptophan proteins, benzoquinone, etc. Typically, BTEX and phenolic compounds are associated with HoN and HiA, respectively. Proteins are typical amphoteric compounds, whereas benzoquinone mainly exists in HoA form. It should be noted that the hydrophilic–hydrophobic properties were likely to be influenced by the concentration of organic matter in aqueous solution, as the organic contaminants were present in the aqueous environment at trace concentrations.

Hydrophilic components in the raw water were mainly composed of phenolic compounds, which were effectively removed after Fenton treatment. The increase in C3 intensity in the HiB fraction was related to the production of soluble microbial products. Because BTEX is resistant to chemical and biological oxidation, the hydrophobic fraction increased and became the dominant fraction in the Fenton and BAF effluents. The protein-like substances were degraded after ozonation, which resulted in a decrease in the HoB fraction. BTEX in the form of HoN was retained owing to its high antioxidative capacity. The BTEX was removed through hydrophobic interaction with biopolymers of the activated sludge after A/O treatment, hence the HoN fraction decreased significantly. Meanwhile, HiA and HiN increased, which might be because tryptophan-like proteins related to biological activity were generated. It was observed that C4 was related to fulvic acids, which area typical natural organic matter and soluble in both acids and bases. The fulvic acids were efficiently removed *via* Fenton oxidation, but increased after BAF treatment, suggesting that biological metabolism produced the fulvic substances in the form of HoA and HiA. Owing to the lower oxidative capacity of O_3 in comparison to that of the Fenton process, the fulvic acids were retained in the ozonation effluent. The HoA fraction of fulvic acids might be removed through bioadsorption, thus the hydrophilic fractions were contained in the A/O effluent. It was noted that the MBR performed well regarding all organic matter compounds, which were almost undetectable after MBR treatment.

3. Practical significance

Traditional analytical methods for organic contaminant characterization, such as GC–MS and HPLC-MS, are very time-consuming and costly. Spectroscopic analysis can be readily conducted and can quickly reflect the transformation and removal efficiency of organic contaminants during water treatment. In this work, various spectroscopic methods were used to characterize the changes in organic contaminants in CTL wastewater during an integrated chemical oxidation and biological treatment process. Based on known organic pollutants in wastewater, EEM-PARAFAC performed better in semiquantitative analysis of the characteristic organic contaminants in CTL wastewater at different treatment stages in comparison to other spectroscopic methods, such as UV–vis and FT-IR. The specific fractionated fluorescent components were related to characteristic organic pollutants. For instance, C1 was associated with humic substances and benzopyrene; C2 indicated ketones, quinhydrone, and anilines; C3 was attributed to aromatic substances, such as BTEX, phenols, tryptophan proteins, and PAHs; and C4 reflected fulvic acid. According to the changes in intensities of different fluorescent components, the removal efficiency of typical organic contaminants could be assessed during the wastewater treatment process. It should be noted that fluorescent regions for different organic contaminants were likely to overlap, which could be further separated using the DOM fractionation procedure. Therefore, DOM fractionation in conjunction with EEM-PARAFAC could more precisely monitor water quality evolution. According to this study, the established integrated process for CTL wastewater treatment was effective in removing the characteristic harmful organic contaminants. Although the transformation and removal of organic matter could be evaluated based on EEM-PARAFAC, the biological toxicity of wastewater from different treatment stages should be also considered, as some organic contaminants are highly toxic at trace concentrations, such as naphthalene and benzopyrene. Therefore, more work is needed to understand the relationships between fluorescent components and biological toxicity. In addition, the correlation analysis between different spectroscopic methods is worthy of further study.

4. Conclusions

In this study, several spectroscopic methods were used to explore the transformation and removal efficiency of specific organic pollutants in CTL wastewater during combined chemical oxidation and biological treatment. The following conclusions can be drawn.

(1) DOM fractions varied significantly during the wastewater treatment. The HoA fraction increased after Fenton oxidation, which was attributable to production of small-molecule organic acids. Formation of SMMs caused obvious increase in the HoN fraction under BAF treatment, which decreased after ozonation, and the HiB and HiA components increased. Biodegradable fractions were removed with the A/O treatment, as production of SMMs was related to re-increasing the HoN component. Finally, the organic matter was mineralized in the MBR treatment.

(2) According to UV–vis analysis, peaks with the absorption wavelengths of 280 nm and 254 nm, which are associated with aromatic substances, were detected in the raw water and Fenton-treated water. The aromatic substances, such as benzenes and phenols, were gradually removed and were undetectable after BAF treatment. In addition, the absorption peak at 210 nm, which is related to C-OH, decreased gradually during the integrated process. Furthermore, the peak at 225 nm, which is associated with protein-like substances produced in biological treatment, was significantly reduced and could not be detected in subsequent treatment.

(3) FT-IR analysis revealed that the functional groups of phenols, BTEX, aromatic hydrocarbon, aliphatic acids, aldehydes, and esters were present in the raw wastewater. After Fenton treatment, raw organic matter was oxidized into small molecules, such as aldehydes and/or ketones. Aromatic hydrocarbons were effectively removed after BAF treatment through bioadsorption and biodegradation. Carboxyl compounds and/or aliphatic acids associated with protein-like substances and various organic acids were present in all the water treatment stages. The characteristic peak of esters was reduced and finally could not be detected after the MBR treatment, which also performed well in the removal of phenols and alcohols.

(4) EEM-PARAFAC suggested that four fluorescent components were fractionated: C1 was associated with humic substances and benzopyrene; C2 indicated ketones, quinhydrone, and anilines; C3 was attributed to aromatic substances, such as BTEX, phenols, tryptophan proteins, and PAHs; and C4 reflected fulvic acid. The established integrated chemical oxidation and biological process for CTL wastewater treatment was effective in removing the characteristic organic contaminants.

Acknowledgments

Appendix A. Supplementary data

Supplementary data to this article can be found online at https://doi.org/10.1016/j.jes.2018.04.006.

REFERENCES

Aftab, B., Hur, J., 2017. Fast tracking the molecular weight changes of humic substances in coagulation/flocculation processes via fluorescence EEM-PARAFAC. Chemosphere 178, 317–324.

APHA-AWWA-WEF, 1998. Standard Methods for the Examination of Water and Wastewater. 20th ed. American Public Health Association, Washington, DC.

Bai, L.L., Xi, H.B., Zhou, Y.X., Li, J., Wang, Y.E., 2016. Organic pollutants and fluorescence characteristics of acrylic wastewater. Chin. J. Environ. Eng. 10 (6), 3366–3372 (In Chinese).

Barker, D.J., Stuckey, D.C., 1999. A review of soluble microbial products (SMP) in wastewater treatment systems. Water Res. 33 (14), 3063–3082.

Benito, A., Penades, A., Lliberia, J.L., Gonzalez-Olmos, R., 2017. Degradation pathways of aniline in aqueous solutions during electro-oxidation with BDD electrodes and UV/H₂O₂ treatment. Chemosphere 166, 230–237.

Bu, L., Wang, K., Zhao, Q.L., Wei, L.L., Zhang, J., Yang, J.C., 2010. Characterization of dissolved organic matter during landfill leachate treatment by sequencing batch reactor, aeration corrosive cell-Fenton, and granular activated carbon in series. J. Hazard. Mater. 179, 1096–1105.

Chen, W., Westerhoff, P., Leenheer, J.A., Booksh, K., 2003. Fluorescence excitation-emission matrix regional integration to quantify spectra for dissolved organic matter. Environ. Sci. Technol. 37, 5701–5710.

Chen, Y.Z., He, Q., Yu, D.N., Li, S., Tan, X.M., 2012. Research on the degradation of BaP with potassium ferrate characterized by fluorescence. Spectrosc. Spectr. Anal. 32 (7), 1842–1845 (In Chinese).

Cheng, C., Wu, J., You, L., Tang, J.K., Chai, Y.D., Liu, B., et al., 2018. Novel insights into variation of dissolved organic matter during textile wastewater treatment by fluorescence excitation emission matrix. Chem. Eng. J. 335, 13–21.

Collard, M., Teychené, B., Lemée, L., 2015. Improved quantitative analysis of molecular constituents of wastewater sludge pellets using double-shot thermochemolysis-CGMS. J. Anal. Appl. Pyrolysis 114, 265–272.

Deng, M.J., Zhang, Y., Quan, X., Na, C.H., Chen, S., Liu, W., et al., 2017. Acute toxicity reduction and toxicity identification in pigment-contaminated wastewater during anaerobic–anoxic–oxic (A/A/O) treatment process. Chemosphere 168, 1285–1292.

Feng, L.L., Xi, H.B., Zhou, Y.X., Yang, Q., Song, G.Q., Bai, L.L., et al., 2015. Representation of wastewater from a section of butadiene polymerization by flocculating setting process. Res. Environ. Sci. 28 (9), 1288–1294 (In Chinese).

Ge, L.K., Na, G.S., Chen, C.E., Li, J., Ju, M.W., Wang, Y., et al., 2016. Aqueous photochemical degradation of hydroxylated PAHs: kinetics, pathways, and multivariate effects of main water constituents. Sci. Total Environ. 547, 166–172.

Han, C.Q., Duan, P.T., Liu, Y., Luo, X.S., Ni, X.W., 2010a. Study on the fluorescence spectra characteristic of acetone-water solution. Laser J. 31 (4), 38–40 (In Chinese).

Han, H.J., Li, H.Q., Du, M.A., Ma, W.C., Xu, C.Y., Wang, W., 2010b. Anaerobic/aerobic/biological ammonia removal/coagulation sedimentation process for treatment of wastewater from coal chemical industry. China Water Wastewater 26, 75–77 (In Chinese).

Hara, J., 2017. Oxidative degradation of benzene rings using iron sulfide activated by hydrogen peroxide/ozone. Chemosphere 189, 382–389.

He, M.C., Shi, Y.H., Lin, C.Y., 2008. Characterization of humic acids extracted from the sediments of the various rivers and lakes in China. J. Environ. Sci. 20 (11), 1294–1299.

Hou, B.L., Han, H.J., Jia, S.Y., Zhuang, H.F., Zhao, Q., Xu, P., 2014. Effect of alkalinity on nitrite accumulation in treatment of coal chemical industry wastewater using moving bed biofilm reactor. J. Environ. Sci. 26, 1014–1022.

Huang, H.J., Yuan, X.Z., 2015. Recent progress in the direct liquefaction of typical biomass. Prog. Energ. Combust. Sci. 49, 59–80.

Imai, A., Fukushima, T., Matsushige, K., Kim, Y.H., Choi, K., 2002. Characterization of dissolved organic matter in effluents from wastewater treatment plants. Water Res. 36, 859–870.

Jiang, J., Li, L., Sun, G.X., 2012. Investigation of redox activities of soil humic acids using 3D excitation emission matrix fluorescence spectroscopy. Environ. Chem. 31 (12), 2002–2007 (In Chinese).

Jiang, T., Skyllberg, U., Björn, E., Green, N.W., Tang, J.H., Wang, D. Y., et al., 2017. Characteristics of dissolved organic matter (DOM) and relationship with dissolved mercury in Xiaoqing River-Laizhou Bay estuary, Bohai Sea, China. Environ. Pollut. 223, 19–30.

Kitis, M., Karanfil, T., Wigton, A., Kilduff, J.E., 2002. Probing reactivity of dissolved organic matter for disinfection by-product formation using XAD-8 resin adsorption and ultrafiltration fractionation. Water Res. 36 (15), 3834–3848.

Lenhardt, L., Dramićanin, M.D., 2016. PARAFAC: a tool for the analysis of phosphor mixture luminescence. J. Lumin. 170, 136–140.

Li, W., Nanaboina, V., Zhou, Q.X., Korshin, G.V., 2012. Effects of Fenton treatment on the properties of effluent organic matter and their relationships with the degradation of pharmaceuticals and personal care products. Water Res. 46, 403–412.

Li, W.T., Chen, S.Y., Xu, Z.X., Li, Y., Shuang, C.D., Li, A.M., 2014. Characterization of dissolved organic matter in municipal wastewater using fluorescence PARAFAC analysis and chromatography multi-excitation/emission scan: a comparative study. Environ. Sci. Technol. 48, 2603–2609.

Li, W.T., Jin, J., Li, Q., Wu, C.F., Lu, H., Zhou, Q., Li, A.M., 2016. Developing LED UV fluorescence sensors for online monitoring DOM and predicting DBPs formation potential during water treatment. Water Res. 93, 1–9.

Li, W.T., Cao, M.J., Young, T., Ruffino, B., Dodd, M., Li, A.M., et al., 2017. Application of UV absorbance and fluorescence

indicators to assess the formation of biodegradable dissolved organic carbon and bromated during ozonation. Water Res. 111, 154–162.

Liu, Y.C., Zhang, G.M., Fang, S.Y., Chong, S., Zhu, J., 2016. Degradation of aniline by heterogeneous Fenton's reaction using a Ni-Fe oxalate complex catalyst. J. Environ. Manag. 182, 367–373.

Louvet, J.N., Homeky, B., Casellas, M., Pons, M.N., Dagot, C., 2013. Monitoring of slaughterhouse wastewater biodegradation in a SBR using fluorescence and UV-visible absorbance. Chemosphere 91 (5), 648–655.

Lu, J.R., Wang, X.L., Shan, B.T., Li, X.M., Wang, W.D., 2006. Analysis of chemical compositions contributable to chemical oxygen demand (COD) of oilfield produced water. Chemosphere 62 (2), 322–331.

Maqbool, T., Hur, J., 2016. Changes in fluorescent dissolved organic matter upon interaction with anionic surfactant as revealed by EEM-PARAFAC and two dimensional correlation spectroscopy. Chemosphere 161, 190–199.

Marquès, M., Mari, M., Sierra, J., Nadal, M., Domingo, J.L., 2017. Solar radiation as a swift pathway for PAH photodegradation: a flied study. Sci. Total Environ. 581-582, 530–540.

Nawrocki, J., Kasprzyk-Hordern, B., 2010. The efficiency and mechanisms of catalytic ozonation. Appl. Catal. B Environ. 99, 27–42.

Oloibiri, V., Coninck, S.D., Chys, M., Demeestere, K., Hulle, S.W.H.V., 2017. Characterisation of landfill leachate by EEM-PARAFAC-SOM during physical-chemical treatment by coagulation-flocculation, activated carbon adsorption and iron exchange. Chemosphere 186, 873–883.

Osburn, C.L., Handsel, L.T., Mikan, M.P., Molly, P., Paerl, H., Montgomery, M.T., 2012. Fluorescence tracking of dissolved and particulate organic matter quality in a river-dominated estuary. Environ. Sci. Technol. 46, 8628–8636.

Peng, S.W., Zhang, W.J., He, J., Yang, X.F., Wang, D.S., Zeng, G.S., 2016. Enhancement of Fenton oxidation for removing organic matter from hypersaline solution by accelerating ferric system with hydroxylamine hydrochloride and benzoquinone. J. Environ. Sci. 41, 16–23.

Sahu, O., Rao, D.G., Gopal, R., Tiwari, A., Pal, D., 2017. Treatment of wastewater from sugarcane industry by electrochemical and chemical process: aluminum (metal and salt). J. Water Process Eng. 17, 50–62.

Sgroi, M., Roccaro, P., Korshin, G.V., Greco, V., Sciuto, S., Anumol, T., et al., 2017. Use of fluorescence EEM to monitor the removal of emerging contaminants in full scale wastewater treatment plants. J. Hazard. Mater. 323, 367–376.

Wang, L., Zhou, Y.Y., Sun, Y.M., Yang, G., 1995. Determination of trace aniline, diphenylamine and n-methylaniline by tridimensional fluorescence spectrometry. Chin. J. Anal. Chem. 23 (1), 97–99 (In Chinese).

Wang, H.B., Zhang, Y.J., Xiao, X., Jin, D., Zhao, N.J., Yin, G.F., et al., 2010a. Excitation- emission fluorescence characterization study of the three phenolic compounds. Spectrosc. Spectr. Anal. 30 (5), 1271–1274 (In Chinese).

Wang, H.B., Zhang, Y.J., Xiao, X., Yu, S.H., Yin, G.F., Guo, L.Q., 2010b. Influence factors on characteristic parameters of three-dimensional fluorescence spectra of phenol. China Environ. Sci. 30 (8), 1032–1037 (In Chinese).

Wei, S.C., Shi, L., 2015. The coal-oil industrial layout evaluation based on water footprint theory. Acta Ecol. Sin. 35 (12), 4203–4214 (In Chinese).

Xue, Y.F., Lu, S.G., Fu, X.R., Sharma, V.K., Mendoza- Sanchez, I., Qiu, Z.F., et al., 2018. Simultaneous removal of benzene, toluene, ethylbenzene and xylene (BTEX) by CaO_2 based Fenton system: enhanced degradation by chelating agents. Chem. Eng. J. 331, 255–264.

Yan, Y., Wang, L.T., Lin, Z.G., Xu, J.G., Chen, G.Z., 1995. Three-dimensional fluorescence spectrometry and its application to simultaneous determination of polyaromatic hydrocarbons by detecting total fluorescence intensity. Chem. J. Chin. Univ. 10, 1519–1522 (In Chinese).

Yang, L.Y., Han, D.H., Lee, B.M., Hur, J., 2015. Characterizing treated wastewater of different industries using clustered fluorescence EEM-PARAFA and FT-IR spectroscopy: implications for downstream impact and source identification. Chemosphere 127, 222–228.

Yang, L.Y., Zhuang, W.E., Chen, C.T.A., Wang, B.J., Kuo, F.W., 2017. Unveiling the transformation and bioavailability of dissolved organic matter in contrasting hydrothermal vents using fluorescence EEM-PARAFAC. Water Res. 111, 195–203.

Yue, X.D., Koh, Y.K.K., Ng, H.Y., 2015. Effects of dissolved organic matters (DOMs) on membrane fouling in anaerobic ceramic membrane bioreactors (AnCMBRs) treating domestic wastewater. Water Res. 86, 96–107.

Zhang, Z.H., Xiang, Q., Glatt, H., Platt, K.L., Goldstein, B.D., Witz, G., 1995. Studies on pathways of ring opening of benzene in a Fenton system. Free Radic. Biol. Med. 18 (3), 411–419.

Zhang, Y.L., Yin, Y., Feng, L.Q., Zhu, G.W., Shi, Z.Q., Liu, X.H., et al., 2011. Characterizing chromophoric dissolved organic matter in Lake Tianmuhu and its catchment basin using excitation-emission matrix fluorescence and parallel factor analysis. Water Res. 45 (16), 5110–5122.